Substructure of Inner Dynein Arms, Radial Spokes, and the Central Pair/Projection Complex of Cilia and Flagella

URSULA W. GOODENOUGH and JOHN E. HEUSER
Departments of Biology and Physiology/Biophysics, Washington University, St. Louis, Missouri 63130

ABSTRACT The substructure of the components of the axoneme interior—the inner dynein arms, the radial spokes, and the central pair/projection complex—was analyzed for *Chlamydomonas, Tetrahymena, Strongelocentrotus,* and *Mnemiopsis* using the quick-freeze, deep-etch technique. The inner arms are shown to resemble the outer arms in overall molecular organization, but they are disposed differently on the microtubule and have two distinct morphologies—dyads with two heads and triads with three. The dyads associate with spokes S_3 and S_2; the triads associate with S_1. The spokes form a three-start right-handed helix with a 288-nm rise; the central pair makes a shallow left-handed twist. The spoke heads are shown to be made up of four major subunits; two bind to the spoke shaft and two bind to a pair of central-sheath projections.

Most motile cilia contain outer and inner dynein arms, radial spokes, and a central pair/projection complex. Mutations affecting the assembly of any of these structures can result in immotility (1); therefore, an understanding of ciliary motility must ultimately include a description of the role played by each. There is good evidence that the outer arms participate in powering the beat (2); whether the inner arms are also directly involved in microtubule sliding is less clear (2, 3). The postulated role of the radial spokes in converting microtubule sliding into bending (4) has recently been questioned (5, 6), and the function of the central pair/projection complex is also unknown except that it appears to be capable of rotation (7, 8).

We have recently applied the quick-freeze, deep-etch technique to an analysis of the structure of the outer arms (9, 10), and have documented several features of their construction, not apparent using other forms of electron microscopy, which should be useful in understanding their function. This paper analyzes the components of the axoneme interior by the same technique, and again points out novel features of their architecture.

We show that there are two distinct species of inner arm, one with two heads and one with three, and that these do not overlap with one another in the fashion of the outer arms (10); instead, they fan out into the interdoublet space. We further show that the inner arms bind to the A microtubule with a 24–32–40-nm period rather than the regular 24-nm period of outer arms, with the two-headed species appearing at the first two positions and the three-headed species at the third. Finally, we illustrate intimate relationships between the spoke heads and the central pair projections, and between the spoke shafts and the inner arms, which suggest that the components of the axoneme interior may function as an integrated system.

MATERIALS AND METHODS

Methods for culturing *Chlamydomonas reinhardi* and *Tetrahymena thermophila* and for preparing their axonemes are described in reference 9. Detergent-extracted *Tetrahymena* cells were prepared as described in reference 11. For reactivation of detergent-extracted *Tetrahymena*, the samples were pelleted, applied to the surface of a piece of glutaraldehyde-fixed lung, and mounted on the head of the freezing machine; the pellet of cells was then sprayed with a solution of 1 mM ATP in 30 mM HEPES (pH 7.4), 25 mM KCl, 5 mM $MgSO_4$ using an artist's air brush and, seconds later, dropped onto the surface of a helium-cooled copper block. This brief exposure to ATP minimizes the structural damage that occurs when the cilia of extracted *Tetrahymena* cells are induced to beat in a concentrated suspension. The *pf-23* strain was kindly provided by Dr. Bessie Huang (Baylor College of Medicine, Houston, TX); *pf-14* and *pf-18* were obtained from the *Chlamydomonas* Culture Collection, Duke University, Durham, NC. Sea urchin axonemes (*Strongelocentrotus purpuratus*), kindly provided by Dr. Winfield Sale (Emory University, Altanta, GA), were prepared as described in reference 12. Ctenophores (*Mnemiopsis leidyi*) were collected by the authors at Chilmark, MA; comb rows were dissected from living organisms and their membranes removed as described for protozoan cilia in reference 9.

Sheared axonemes were prepared either by squirting an axoneme suspension repeatedly through a 27-gauge needle or by subjecting it to homogenization in a Virtis apparatus at top speed for 1–2 min. Methods for quick-freezing and deep-etching axonemes were as described in references 9, 10, and 13.

THE JOURNAL OF CELL BIOLOGY · VOLUME 100 JUNE 1985 2008–2018

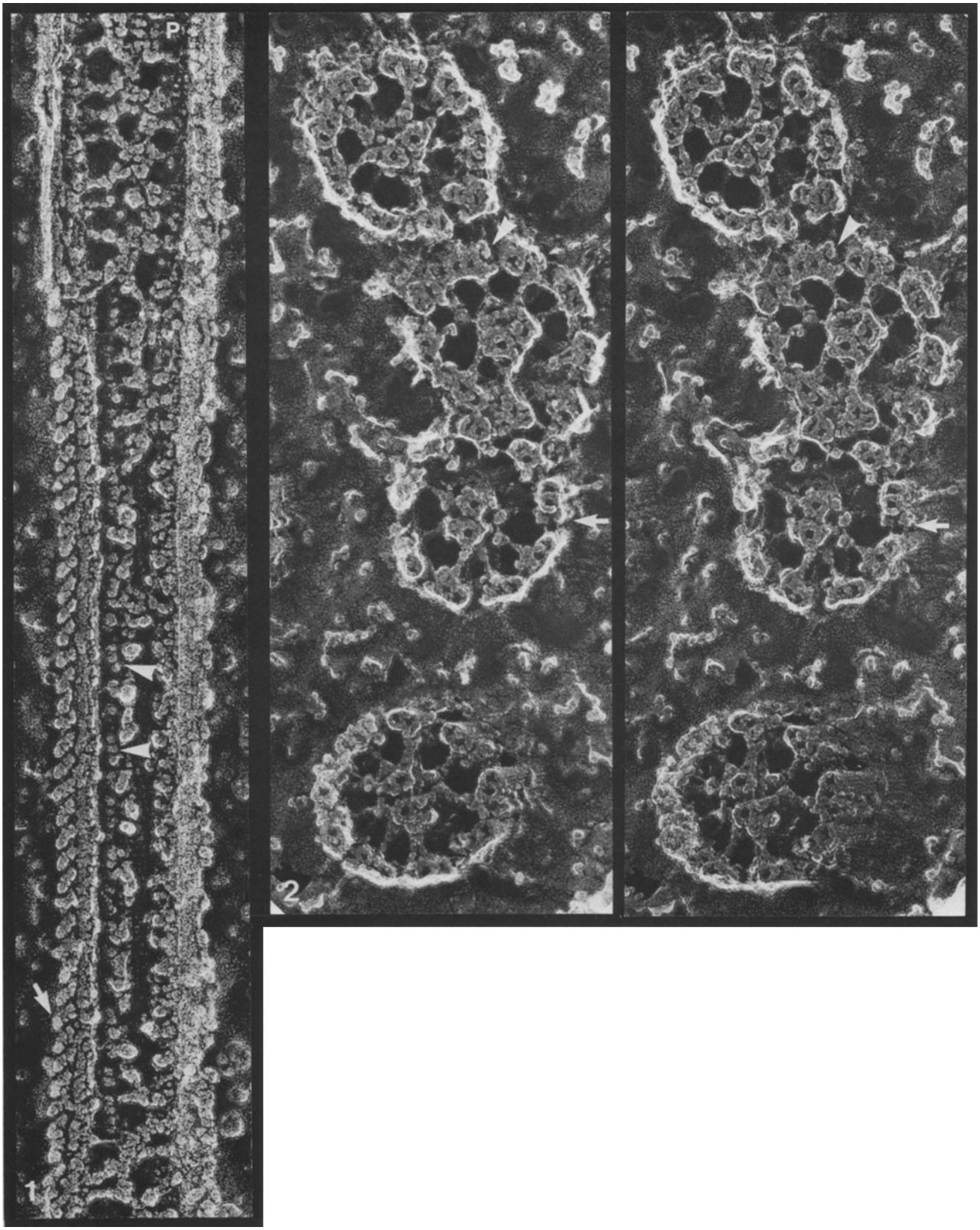

FIGURES 1 and 2 (Figure 1) *Tetrahymena* axoneme (rigor) in longitudinal fracture. A row of outer dynein arms on the left A microtubule is seen from the vantage point of the next B microtubule; we interpret the prominent head (arrow) on each arm to represent the third head which cannot be seen from the axoneme exterior and which creates the "hook" seen in cross section (discussed in reference 10). Clusters of deep inner arm heads are indicated by arrowheads. Longitudinal views of the radial spoke system are included at the top and bottom of the field; cross-fractured spokes appear in the center of the field as groups of irregular white objects. Central-pair projections at *P*. × 185,000. (Figure 2) *Tetrahymena* cilia in cross fracture, stereo pair, from a detergent-extracted cell. The radial spokes associate with the projections which stand up above and below the central pair and associate closely with the sides of the central pair. The helical disposition of the spokes is evident in stereo. Connections between the central-pair microtubules are visible in the bottommost axoneme. Arrow points to a well-preserved set of outer and inner arms showing their stalk connections to the B tubule; arrowhead indicates an outer arm with a prominent "hook." × 165,000.

RESULTS

The Axoneme Interior

Figs. 1 and 2 provide overviews of the axoneme interior as seen in platinum replicas. In Fig. 1, a *Tetrahymena* axoneme has been fractured along its longitudinal axis. A row of outer arms, seen from the perspective of the contiguous B tubule, is seen at the left. At the top and bottom of the field, triplet spoke units are seen extending from the central-pair projections (*P*) to the outer doublets; in the middle of the field, the spokes have been fractured off, leaving irregular white stubs. The inner arms on the left side appear as recessed, barely discernible globular objects (arrowheads); those on the right have been badly distorted by fracturing. Fig. 2 provides a stereo view of axoneme interiors of *Tetrahymena* cilia in cross fracture; the image bears a close correspondence to the familiar thin-section view.

Figs. 1 and 2 illustrate the difficulties encountered in analyzing the axoneme interior by deep-etching: the axoneme must by definition by fractured open, and the structural damage resulting from this fracture is often severe; moreover, when the components of interest are deep within the curved axoneme, they are often inadequately exposed by etching and/or inadequately replicated. In the figures that follow, these difficulties have to varying degrees been overcome, either by fortuitous fractures or by shearing open the axonemes and allowing their components to adsorb to mica flakes (13). We will first analyze images of the central pair/projection complex and the radial spokes, and then turn to the inner arms.

Central Pair/Projections

When cilia are demembranated, the central pair/projection complex often separates from the axonemal doublets (14, 15). Fig. 3 shows such a splaying axoneme adsorbed to a mica flake. When viewed in stereo, the central pair is seen to assume a shallow left-handed twist (cf. reference 7), allowing its overlying projections to be viewed from several vantage points. At the top of the field (region 1), the projections contact to form a tent over the microtubules, much as is observed in cross section (Fig. 2 and references 14, 16, and 17). In region 2, this tent has either collapsed or has been fractured off, revealing the central pair lying side-by-side. In region 3, the central pair twists such that the leftward microtubule comes to lie above the right; here the projections are seen closely applied to the microtubule wall. At the bottom of the field (region 4), the projections form a tent to the left side of the pair.

The projections, which display a 16-nm period (18), are seen to advantage in Fig. 4, where a released central pair has adsorbed directly to mica and has been partially fractured. Each projection is a linear structure, 20 × 7 nm, which binds to the microtubule at its proximal terminus and displays a slight swelling at its distal terminus.

It has previously been reported that a second system of projections, carried by the C_1 member of the central pair, has a 32-nm repeat. These projections have been described for both rat sperm flagella (19) and for *Tetrahymena* cilia (20). Fig. 5 illustrates the apparently homologous system carried by *Chlamydomonas*. Shown is a single central-pair microtubule carrying the standard 16-nm projections along the bottom right and the 32-nm system along the top. Each projection forms a triangle or "barb" (19), with a prominent knob at the apex and two bifurcating fibrils that contact the microtubule wall. A curious feature of this system is that we have yet to identify its counterpart in deep-etched axonemes, nor in disrupted axonemes that have adsorbed to mica; it has only been visualized when isolated flagella, not exposed to detergent, are adsorbed to mica. An obvious inference is that the 32-nm projections are labile to detergent, but we have not pursued this question further.

Radial Spokes

Warner (21) and Warner and Satir (4) have published excellent thin-section images of the radial-spoke system, and Huang, Luck, Piperno, and Ramanis have provided an elegant analysis of radial-spoke composition, showing the spoke head to be constructed from five to six different polypeptides and the spoke shaft from eleven to twelve others (for review see reference 1). Although deep-etching does not shed new light on the morphology of the shaft, it does reveal the substructure of the head and its interaction with the sheath.

Fig. 6 shows a row of spokes attached to a *Tetrahymena* doublet. The triplet clusters of spokes (S_1–S_3) repeat at precisely 96 nm, with 24 nm separating S_3 from S_2, 32 nm separating S_2 from S_1, and 40 nm between S_1 and the S_3 of the next cluster. Viewed from the side, as in Fig. 6, each spoke head measures ~24 × ~9 nm and is composed of a central globular unit (large arrow) flanked by two lateral units (arrowheads). The span of the lateral units can vary; those marked with small arrows in Fig. 6 are widely displaced, giving the spoke head a mushroom shape. When the spoke heads are viewed *en face*, as in Fig. 7, each is seen to be a tetramer, with two central globular units (arrows) flanked by the two lateral units.

Each spoke head contacts two central-sheath projections by its two lateral domains (Figs. 8 and 9, arrows). Since the 24–32–40 spacing of the spokes is not in strict alignment with the 16-nm spacing of the projections, these interactions necessitate a distortion of the system. Both the spokes and the projections prove to be designed to accommodate the mismatch: the spoke heads can extend out to contact the projec-

FIGURES 3–5 (Figure 3) *Chlamydomonas* axoneme adsorbed to polylysine-treated mica, stereo pair. See text for description. ×100,000. (Figure 4) *Tetrahymena* central pair, from an axoneme preparation squirted through a needle in the presence of ATP before adsorption to mica. The two central-pair microtubules are visible at the left, connected by faint striations (arrow). These have then been fractured to reveal their underlying projections spaced at 16 nm. Arching above the central pair are triple sets of spoke heads (one set is labeled *S*); presumably a row of spokes lost its contact with this central pair, adsorbed to the mica via its spoke heads, and was then fractured near the head/shaft junction. The sets denoted with arrowheads are enlarged in stereo in Fig. 7. × 170,000. (Figure 5) Single central-pair microtubule from a preparation of *Chlamydomonas* flagella that were not exposed to detergent, some of which blebbed off their membranes during sample preparation. The projections on the lower right surface have the 16-nm repeat of the sheath; the barbed elements on the upper surface display a 32-nm repeat. × 200,000.

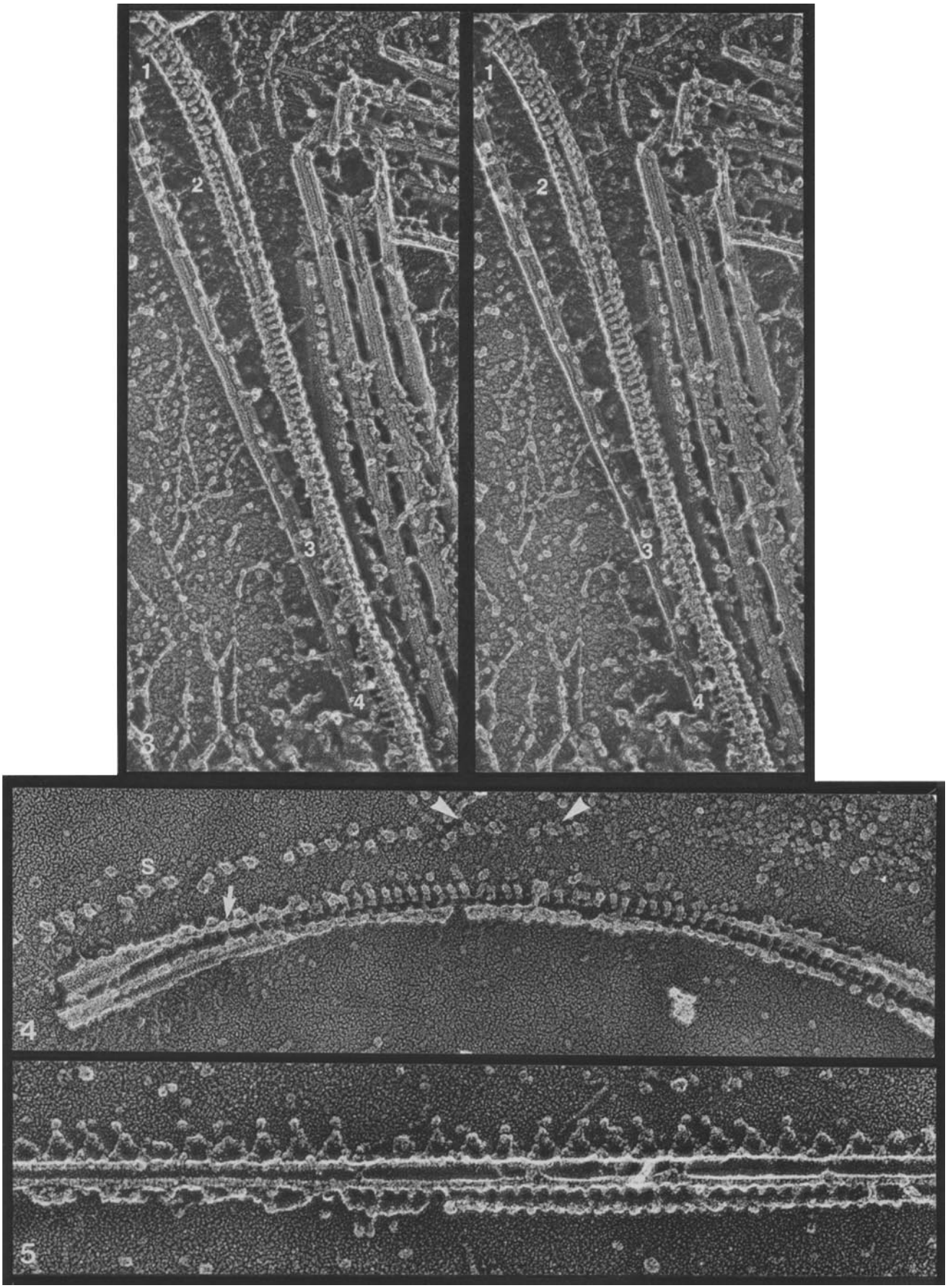

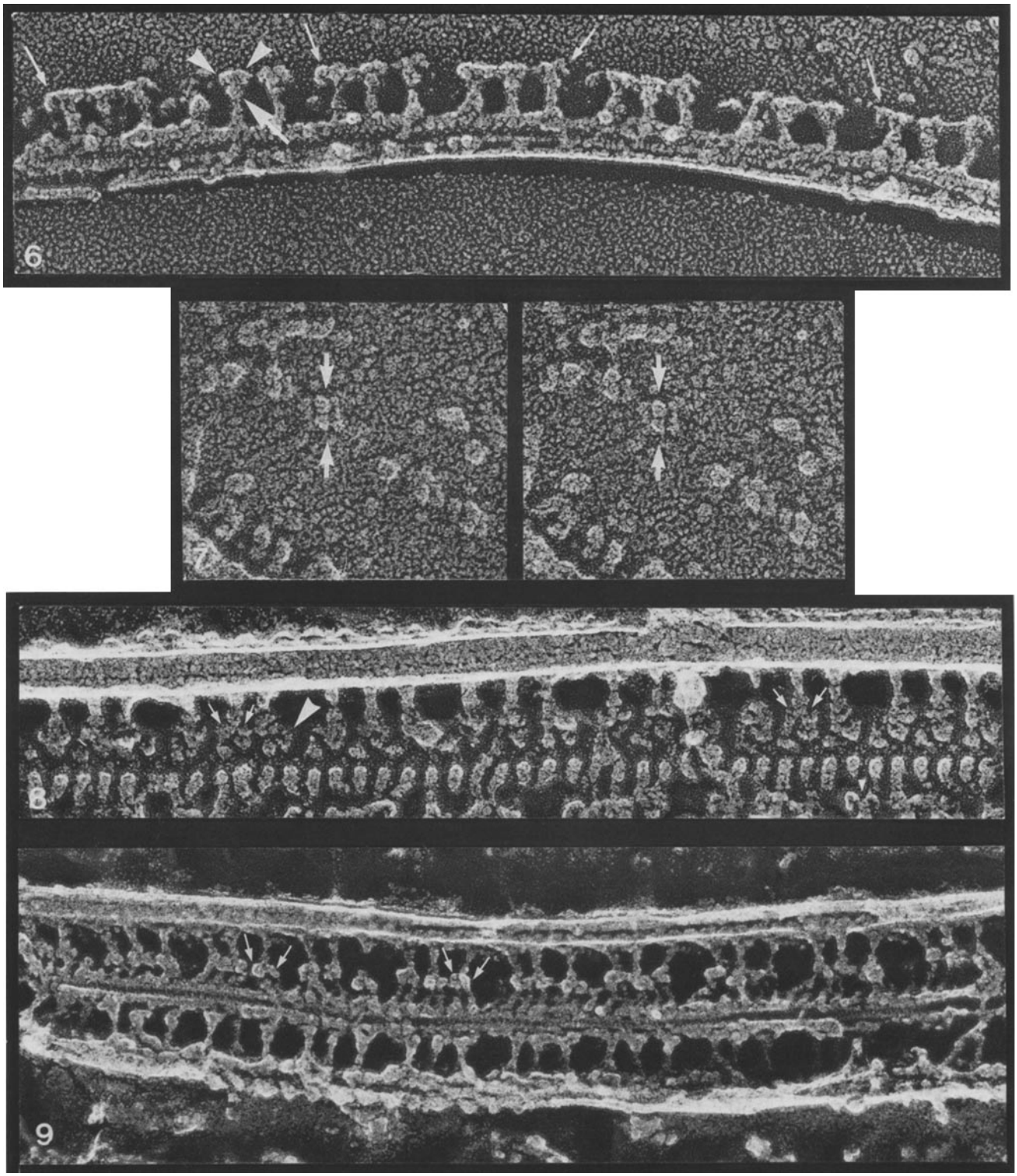

FIGURES 6–9 (Figure 6) *Tetrahymena* doublet with attached radial spokes, prepared as described for Fig. 4. Each spoke head has a central domain (large arrow) and two lateral domains (arrowheads), one facing proximally (right) and the other distally (left). Several of the lateral domains adopt a hook shape (small arrows). Side-to-side contact between heads is also possible via these lateral domains. × 270,000. (Figure 7) Six *Tetrahymena* spoke heads, stereo pair, enlarged from the region denoted with arrowheads in Fig. 4. Each head displays four domains. The two prominant globular subunits in the center of each head (arrows) normally contact the spoke shaft (which has been fractured away), and correspond to the central spoke-head domains in Fig. 6. The less prominent domains, which lie closer to the mica, normally contact the central-pair projections and correspond to the lateral domains in Fig. 6. × 350,000. (Figure 8) Interior of a *Tetrahymena* axoneme incubated in 1 mM ATP plus 50 μM sodium vanadate. Base of the cilium is to the left. In the foreground is a set of 16-nm projections. Several of its associated spoke heads are visible at the lower right; the head marked with a small arrowhead displays the lateral hooks noted in Fig. 6. In the background is a row of radial spokes associated with a second set of projections. Arrows designate cases that show the one-to-one association between a projection and a lateral domain of a spoke head. Large arrowhead shows an example where an S_3 head has pulled a projection leftward from its usual position on the lattice. × 250,000. (Figure 9) *Tetrahymena* axoneme from a detergent-extracted cell sprayed with 1 mM ATP just before freezing. Many of the cilia on this cell were curved and their arms tilted, suggesting it was frozen in mid-beat. Base of the cilium is to the right. Triple groups of spokes pull in towards one another with a concomitant bunching of the central-pair projections. Arrows indicate the one-to-one association between projections and the lateral domains of the spoke heads. × 200,000.

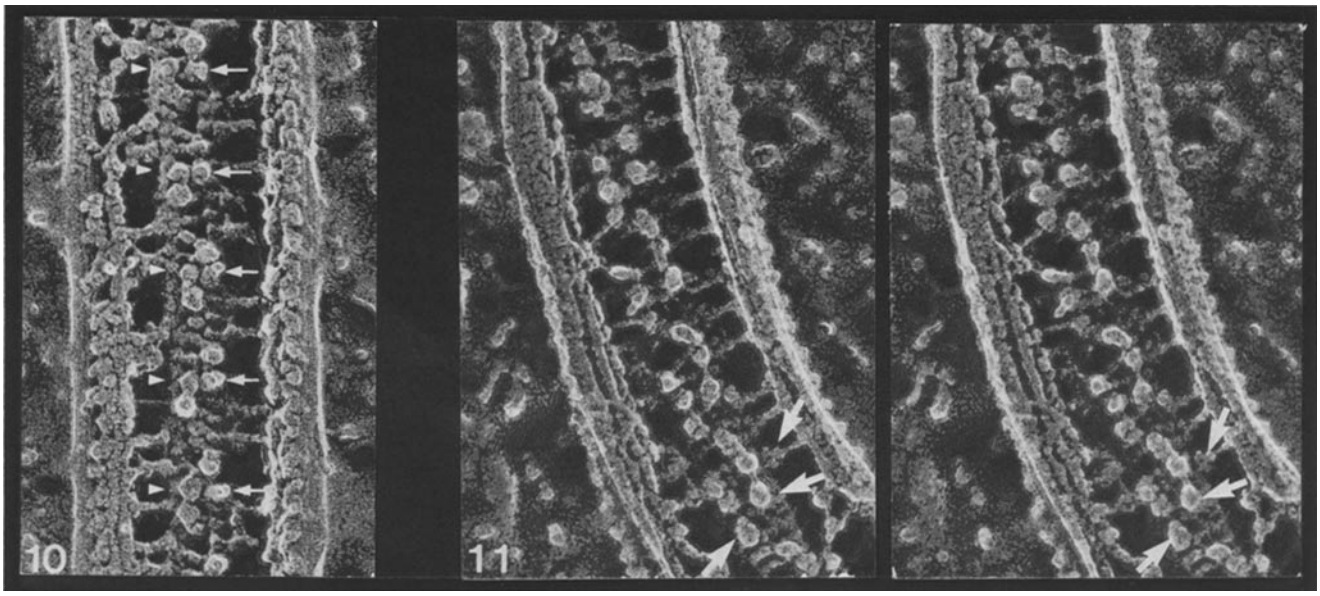

FIGURES 10 and 11 Helical organization of the radial spoke system of *Chlamydomonas* (Fig. 10) and *Tetrahymena* (Fig. 11, stereo pair). Adjacent sets of two (Fig. 10) or three (Fig. 11) spokes form a right-handed helix as they ascend around the central pair, with an incremental rise of 32 nm. In Fig. 10, S_1 spokes of the leftward set are indicated by arrowheads, and S_2 spokes of the rightward set are indicated by arrows. In Fig. 11, arrows indicate three successive S_1 heads. (Fig. 10) × 140,000; (Fig. 11) × 170,000.

tions, and the projections can be displaced by spoke attachments (Fig. 8, arrowhead). In general, therefore, the projections and the spokes can both be thought of as hinged elements, anchored with a precise spacing at their microtubule binding sites, but flexible at their distal ends.

An intriguing example of this flexibility has been found in preparations of detergent-extracted *Tetrahymena* cells (11) reactivated with 1 mM ATP. As shown in Fig. 9, the radial spoke heads cluster together, so that although spokes S_1 and S_3 of a given triplet continue to be separated by 56 nm at their A-tubule binding sites, their heads are separated by 48 nm or less. Accompanying this change, the projections associated with the S_1 heads are pulled in from the right and those associated with S_3 are pulled in from the left. Evident also in Fig. 9 is an inward cant adopted by several of the spoke shafts, a phenomenon first observed in situ by Warner and Satir (4).

Although most cilia bear spokes in groups of three, there are cilia wherein the spokes occur in pairs, examples being the sperm tails of *Sarcophaga* (blowfly) (19) and the flagella of *Chlamydomonas* (14). The spoke pairs repeat every 96 nm, like the triplets of other organisms, and the members of each pair are separated by 32 nm. Hence the spoke-pairs are equivalent to spokes S_1 and S_2 of the triple-spoke systems; the more narrowly spaced S_3 is missing.

When straight regions near the base of the axoneme are examined, the 96-nm spoke repeat on one A microtubule is staggered upward by 32 nm with respect to its leftward neighbor. This pattern is illustrated in Fig. 10. The arrowheads indicate the S_1 spokes along one *Chlamydomonas* doublet, and the arrows indicate the S_2 spokes along the adjacent doublet. The arrowheads are in register with the arrows, indicating that each spoke pair is displaced by 32 nm relative to its neighbor. In curved regions of the axoneme this pattern can shift, as would be expected if one doublet has slid past its neighbor. Thus in the *Tetrahymena* cilium shown in Fig. 11, which was exposed to ATP, the spokes at the base of the field are staggered by the expected 32 nm (arrows), whereas the stagger increases towards the top of the field as the axoneme curves.

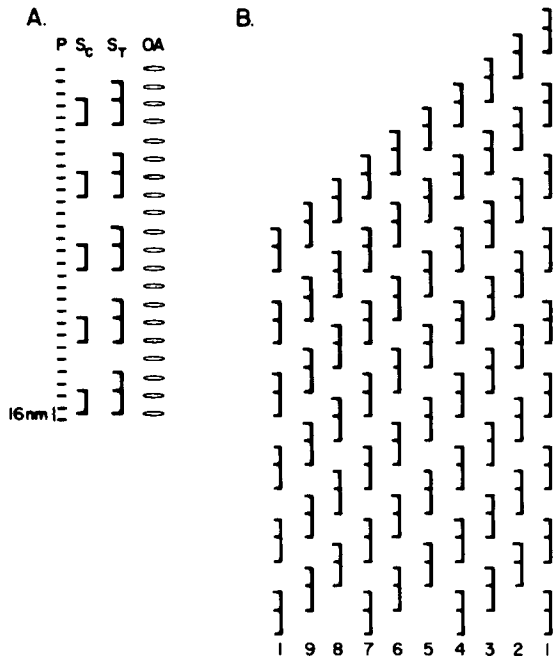

FIGURE 12 (*A*) Diagram of the spatial relationships between the central-pair projections (*P*), the spoke systems of *Chlamydomonas* (S_C) and *Tetrahymena* (S_T), and the outer arms (*OA*). (*B*) Diagram of the three-start right-handed helix formed by the radial spoke system in *Tetrahymena*. Spoke S_3 is absent from the otherwise equivalent system of *Chlamydomonas*.

Fig. 12 diagrams the topology of the full spoke system. It has the form of a three-start (or two-start for *Chlamydomonas*) right-handed helix with a 288-nm pitch.

Inner Arms In Situ

Fig. 13 shows the interior of a *Tetrahymena* axoneme which opened out into a flat sheet during the course of dialysis

against a low ionic strength solution containing EDTA. Although individual inner arms prove to be in considerable disarray in such opened-out axonemes, the images provide a good overview of the inner-arm system. In Fig. 13, the radial spokes have been fractured near their origin and appear as groups of three white knobs. The inner-arm system is particularly in evidence along the doublet marked with the large arrows, where it appears as clusters of spherical objects (arrowheads) which lie just to the left of the A microtubule and attach to the leftward B microtubule via narrow stalks (small arrows).

Fig. 14 shows a comparable opened-out axoneme from the *pf-14* mutant of *Chlamydomonas*, which lacks radial spokes (22). The inner arms, no longer shielded from view by the spokes, are again seen to bind to the B tubules by slender stalks (arrows). Their globular domains again lie in the interdoublet space just to the left of the A tubules; individual examples will be presented at higher magnifications below. The point of this figure is to show that the interior of the axoneme is literally packed with inner arms.

Figs. 15–21 show inner arms in intact cylindrical axonemes that have been fractured open after quick-freezing. Because of the geometry of the system, a replica with optimal views of the stalks (e.g., Fig. 15, arrows) proves to bear poor examples of the globular elements, whereas replicas with optimal views of the globular elements (Figs. 16–21) are oriented such that the stalks are not in view.

The overall design of the inner arm, diagrammed in Fig. 22, proves to be homologous to the outer arm (10): domains we designate as "feet" bind to the A microtubule, corresponding to the A-binding feet of the outer arm; domains we designate "heads" attach to the feet via narrow "stems," much as the outer arm heads attach to their feet via stems; and the heads in both cases attach to the B microtubule via the above-mentioned "stalks." There are, however, four important differences between the outer and inner arms.

First, whereas there is only one morphological form of outer arm, there are two distinct morphological forms of inner arms: dyads with two heads, and triads with three. (In Figs. 16–19, dyads are designated by D and triads by T, and arrows indicate examples wherein the double or triple heads are particularly well preserved; in Figs. 20 and 21, the triads are indicated by vertical bars).

Second, the dyads and triads alternate in a regular pattern: two dyads, one triad, two dyads, one triad, and so on. (This pattern is indicated by the D-D-T repeats in Figs. 16–21.)

Third, the dyad-dyad-triad grouping repeats every 96 nm, exactly the repeat of the radial spokes, with dyad 1 aligning with spoke S_3, dyad 2 aligning with S_2, and the triad aligning with S_1. This association of the inner arms with the spoke system is suggested by Fig. 13, where the inner arms are confined to the same domains of the axoneme as the spokes, and is directly documented in Fig. 16, where three spoke stubs (labeled 1–3) underlie each D-D-T unit. Interestingly, this period is also found in wild-type *Chlamydomonas* (Fig. 21), which has only the S_1 and S_2 spokes, and in the *pf-14* mutant of *Chlamydomonas* (Fig. 20), which has no spokes. Therefore, it is apparently autonomous to the inner arms.

Fourth, the inner arms are disposed on the microtubule in a very different fashion from the outer arms: their component heads radiate out into the interdoublet space, whereas the outer arm heads reach over to the feet of their proximal neighbor, adopting what we have recognized to be an overlap configuration (10).

Since the inner arms have the same period as the spokes, it is in some cases difficult to determine whether material associating with the A microtubule represents the base of an inner arm or a fractured-off spoke. This ambiguity does not arise in the case of the spokeless *pf-14* mutant, however, and Figs. 14, 15, and 20 demonstrate that, even here, A-associated material associates with the inner arm.

DISCUSSION

Our study documents what Warner has previously suggested (19), namely, that the primary vernier of the axoneme appears to be the 4-nm lattice of the microtubule. Thus, as diagrammed in Fig. 22, the central-pair projections repeat at 16 nm (with a second set repeating at 32-nm); the spokes and the inner arms repeat at 24, 32, and 40 nm; and the outer arms repeat at 24 nm. The most straightforward way to imagine how these periodicities are established during flagellar biogenesis is to propose that the various protofilaments of flagellar microtubules carry binding sites for different components, a proposal which only serves to push the issue back to the question of how protofilaments could be so differentially programmed. Since we find that the inner arms associate correctly with the *Chlamydomonas* A microtubules even when all visible components of the spokes have been deleted by gene mutation (Figs. 14, 15, and 20), the inner-arm binding sites are apparently not the spokes per se. Nevertheless, in normal axonemes, spoke binding sites and inner arm binding sites are in register; hence it is hard to know which is primary.

Our replicas have thus far failed to yield images of anything that might correspond to "nexin" or "interdoublet links," which others have described as internal strands that extend from A to B microtubules with a 96-nm period (20, 23). The problem does not appear to be caused by obscuration of such links by spokes or inner arms, since we also fail to see links in the spokeless *pf-14* mutant (Figs. 14, 15, and 20) or in the inner arm–less mutant, *pf-23* (not shown). The nexin image in intact axonemal cross sections could well be generated by the stem and stalk domains of inner arms (Fig. 2, arrow). Reports of nexin links with a 96-nm period have been based on observations of axonemes extracted with high salt (20, 23). Possibly, one of the inner arms in each 96-nm grouping is resistant to salt extraction and instead denatures to create the nexin image. Otherwise, we have no explanation for this one discrepancy between thin-section and quick-frozen images of axoneme interiors.

That the inner arms have several heads is evident in the thin-section micrographs published by Tilney et al. (24), and is specifically noted by Haimo et al. (25). It is intriguing that sea urchin outer arms have two heads (26), that *Chlamydomonas* and *Tetrahymena* outer arms have three heads (11, 27), and that all three organisms have both two-headed and three-headed inner arms (present study). If one postulates that each type of head is composed of a distinct heavy chain, then there would be two species per dyad and three species per triad, a total of five; Huang et al. (3) find that six heavy-chain species are deficient in the inner arm–defective mutant, *pf-23*. It is also intriguing that in all cilia thus far examined, the outer arms overlap one another whereas the inner arms do not. Clearly the two types of arms must be specified by genes that have common ancestors, but their different dispositions on the microtubule suggest that they may carry out unique

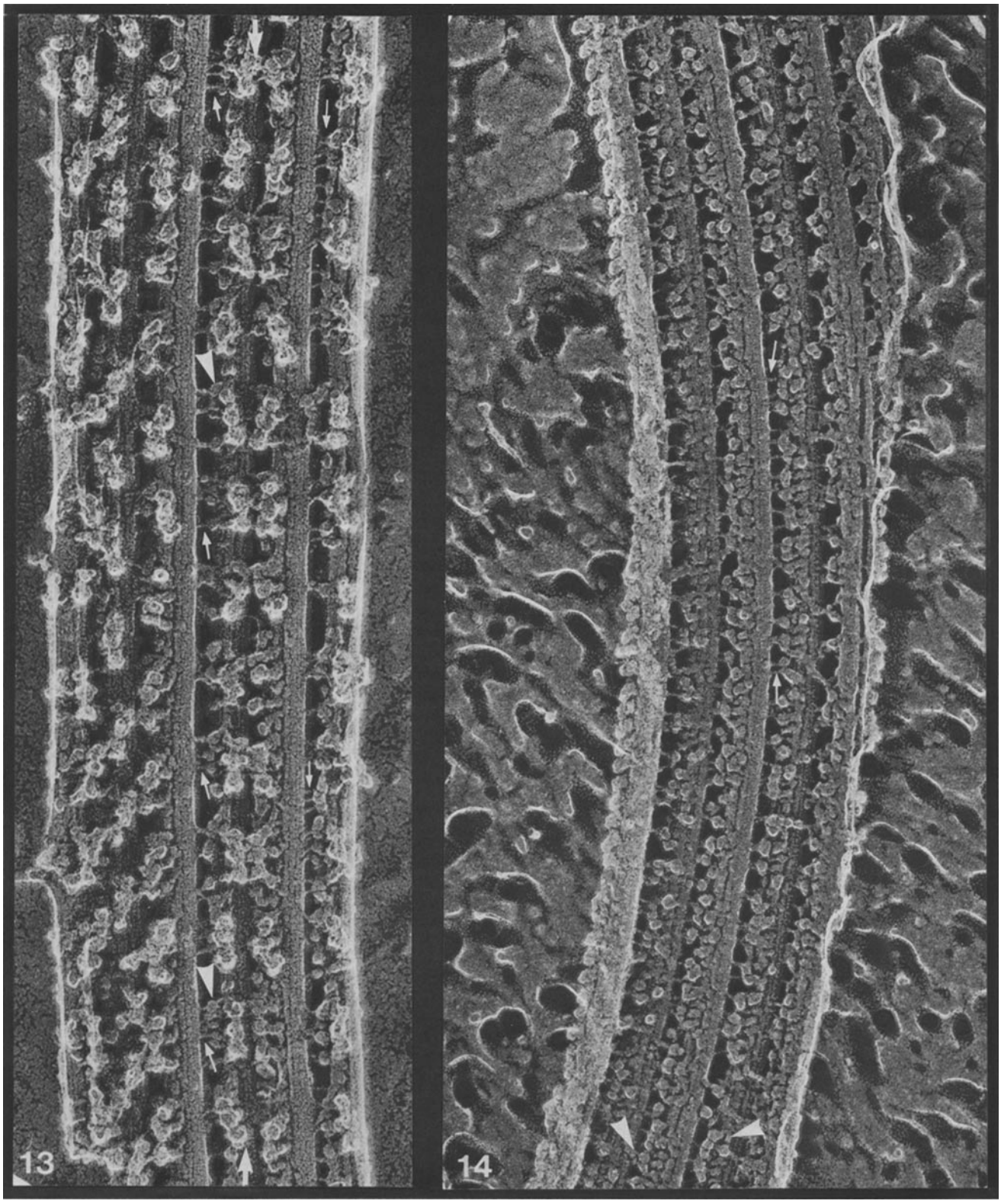

FIGURES 13 and 14 (Figure 13) Opened-out *Tetrahymena* axoneme subjected to overnight dialysis against Tris-EDTA (20). Large arrows mark doublet displaying optimal clusters of inner arms; these attach to the adjacent B tubule by slender stalks (small arrows) and associate with the A tubule via bulky domains (arrowheads). Radial spokes, fractured near their heads, appear as white clusters along the A tubules. Note that the helical alignment between sets of radial spokes (cf. Fig. 12) is preserved along the leftward three doublets, whereas the spokes are aligned in register along the rightward three doublets, an example of the shift in spoke alignment that accompanies shifts in doublet alignment (the shift here presumably accompanying or the consequence of the "opening-out" event). × 125,000. (Figure 14) Opened-out *Chlamydomonas* axoneme of the *pf-14* strain lacking radial spokes. An optimal group of inner arm stalks attached to a B microtubule is marked by arrows; bulky domains associate with the rightward A tubule, and discrete globular heads lie in the interdoublet gap. Arrowheads point to distinct double-headed and triple-headed species. Row of outer arms is visible along the leftmost doublet (cf. Fig. 1). × 140,000.

functions in the modern axoneme.

High-speed cinematography has been used to analyze the residual motility displayed by mutant strains that lack components of the axoneme interior. Brokaw et al. (6) document that in the spoke head–less *pf-17* mutant combined with different sup_{pf} suppressor mutations, the stroke intiates with a large-amplitude principal bend. The flagellum then typically develops one or more secondary reverse bends and, as these propagate, the flagellum flops over to the opposite side of the cell, which it never does during its normal asymmetric cycle. Goldstein (28) demonstrates that in the *pf-18* mutant, whose central-pair microtubules are replaced by a core of dense material (17), the bends that form tend to have a smaller amplitude than normal—they are deflections rather than true curves—and although some begin to propagate, they usually straighten out before propagation has progressed very far along the axoneme.

The properties of these mutant wave forms suggest that one

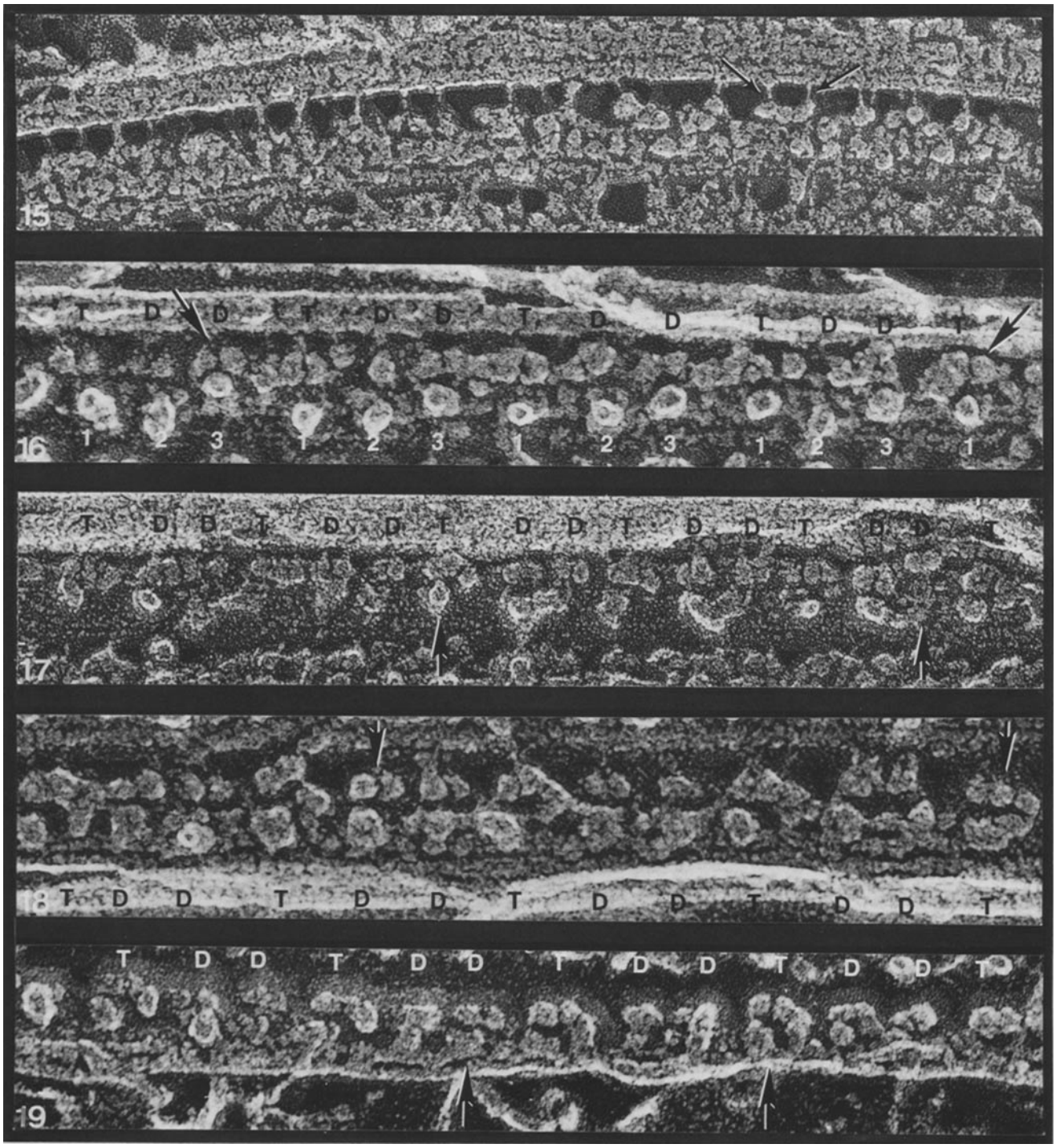

FIGURES 15–19 Rows of inner arms in rigor axonemes. Dyad (two-headed) arms are designated D; triad (three-headed) arms are designated *T*. Arrows indicate examples in each row whose morphology is particularly well preserved. (Fig. 15). *Chlamydomonas pf-14* mutant, showing inner arm stalks (arrows). × 270,000. (Figure 16) Ctenophore comb row; spokes S_1–S_3 are labeled *1–3*. The leftmost triad and two rightmost dyads are not well preserved. × 350,000. (Figure 17) Sea urchin sperm tail. × 350,000. (Figure 18) Sea urchin sperm tail. × 440,000. (Figure 19) Ctenophore comb row. × 440,000.

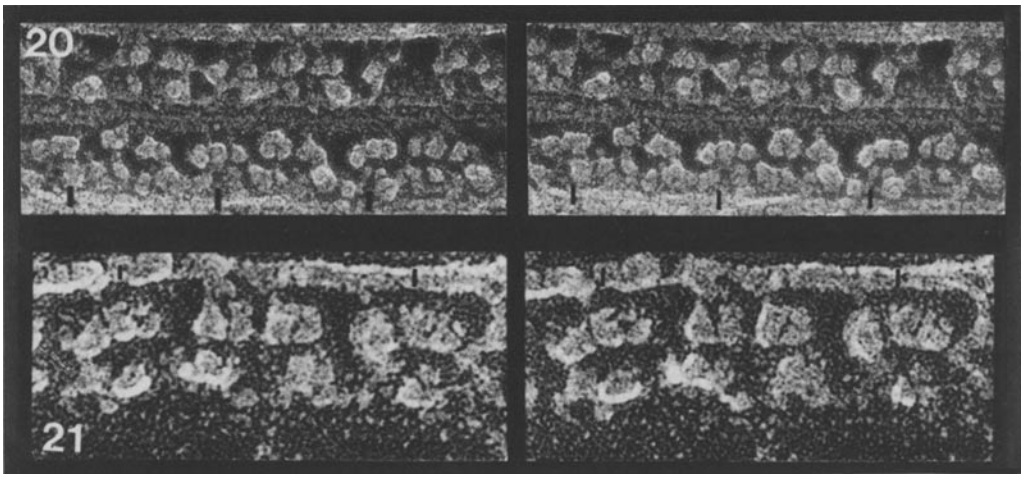

FIGURES 20 and 21 Stereo views of *Chlamydomonas* inner arms in rigor axonemes. Triad positions are indicated by bars. (Figure 20) *pf-14* mutant. × 230,000. (Figure 21) Wild-type. × 390,000.

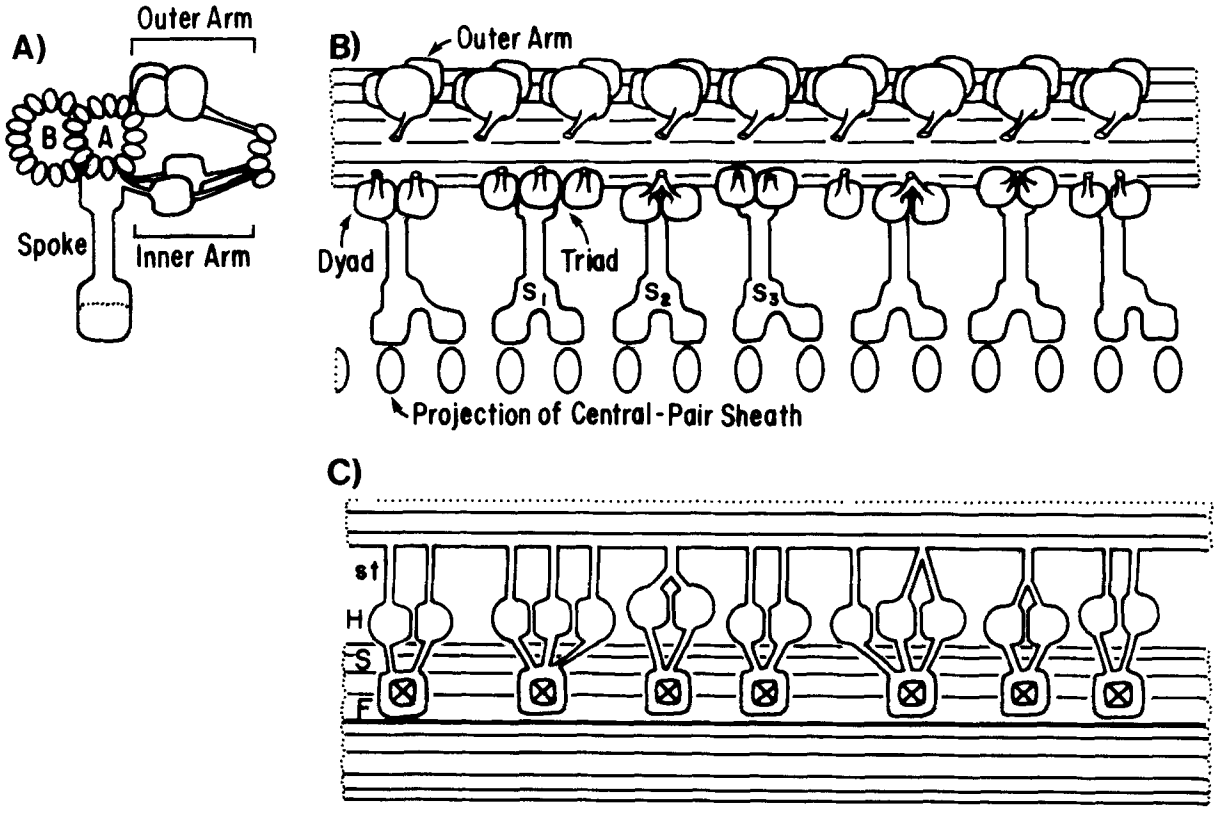

FIGURE 22 (*A*) Diagram of a ciliary doublet and a set of outer and inner arms in cross section. The superimposition of several inner arm heads, each with a variable position in the interdoublet gap, presumably explains the indistinct morphology of the inner arm in thin section (24, 25). The strands connecting the heads to the microtubules follow the same course as "nexin links." (*B*) Diagram of inner arm-deployment from the vantage point of the contiguous B microtubule, to which the cut-off stalks would ordinarily bind. The dyad inner arms are in register with the outer arms and with the S_3 and S_2 spokes spaced at 24 nm, whereas the triad inner arms, although centered over S_1, span the positions occupied by two outer arms. The mismatch between the radial spoke period and the central-pair projections is drawn as being resolved by a deflection of the spoke head, but as noted in the text, the projections may also shift. (C) Dyad (two-headed) and triad (three-headed) inner arms viewed *en face*, as in Figs. 15–21. Spokes would extend straight out toward the viewer; their positions are marked with X's over the A-binding feet (*F*) of the inner arms. *S*, stem; *H*, head; *st*, stalk.

of the functions of the central pair/spoke system may be to serve as a spring; that is, as a device that returns to its original form after being forced out of shape. Thus the dynein-mediated sliding of a subset of the nine outer doublets may itself generate a bend, but the shape and mechanical properties of that bend may be defined by its deflection of the central spring, a deflection that may occur in quantal steps (29). Of interest in this regard are the properties of the flagellum of the eel spermatozoan, which lacks both outer arms and the central pair/spoke system and generates helicoidal rather than planar waves (30). Without the buttress of a central spring, axonemal sliding may generate a twist which, when propagated, generates a helical torque to the flagellum.

Several investigators have concluded that the radial spoke system forms a helix (4, 15, 19), but it has not been clear whether a helical pattern is assumed in straight regions only, in curved regions only, or in both. We have measured a three-start (or two-start for *Chlamydomonas*) right-handed helix with a 288-nm rise (Figs. 10 and 12) at the base of straight, rigor axonemes where sliding displacement would not be expected to have occurred. We also show that the pitch of this helix can change during bend formation (Fig. 11), and that major distortions can occur if axonemes splay open during sample preparation (Fig. 13; cf. reference 15). We further confirm the observation of Omoto and Kung (7) that the central pair makes a shallow left-handed helix within the axoneme. If these helices indeed constitute a ciliary spring, then such information should assist in deducing its mechanical properties.

We thank Dr. Win Sale for sea urchin axonemes, Carol Hwang for cell cultures, Robyn Roth for the replicas, Lori van Houten for photography, Ann Dillon for drawings, and Amy Papian for typing.

This work was supported by grant GM-33835 from the National Institutes of Health.

Received for publication 11 December 1984, and in revised form 1 March 1985.

Note added in Proof: Warner et al. (*J. Cell Sci.*, 1985, in press) have observed that when isolated inner arm dynein from *Tetrahymena* is added back to dynein-extracted axonemes, it preferentially binds at the bases of the radial spokes.

REFERENCES

1. Luck, D. J. L. 1984. Genetic and biochemical dissection of the eucaryotic flagellum. *J. Cell Biol.* 98:789–794.
2. Gibbons, B. H., and I. R. Gibbons. 1973. The effect of partial extraction of dynein arms on the movement of reactivated sea-urchin sperm. *J. Cell Sci.* 13:337–357.
3. Huang, B., G. Piperno, and D. J. L. Luck. 1979. Paralyzed flagellar mutants of *Chlamydomonas reinhardtii* defective for axonemal doublet microtubule arms. *J. Biol. Chem.* 254:3091–3099.
4. Warner, F. D., and P. Satir. 1974. The structural basis of ciliary bend formation: radial spoke positional changes accompanying microtubule sliding. *J. Cell Biol.* 63:35–63.
5. Huang, B., Z. Ramanis, and D. J. L. Luck. 1982. Suppressor mutations in Chlamydomonas reveal a regulatory mechanism for flagellar function. *Cell.* 28:115–124.
6. Brokaw, C. J., D. J. L. Luck, and B. Huang. 1982. Analysis of the movement of *Chlamydomonas* flagella: the function of the radial-spoke system is revealed by comparison of wild-type and mutant flagella. *J. Cell Biol.* 92:722–732.
7. Omoto, C. K., and C. Kung. 1980. Rotation and twist of the central pair microtubules in the cilia of *Paramecium*. *J. Cell Biol.* 87:33–46.
8. Kamiya, R. 1982. Extension and rotation of the central-pair microtubules in detergent-treated *Chlamydomonas* flagella. *Cell Motility.* 1(Suppl.):169–173.
9. Goodenough, U. W., and J. E. Heuser. 1982. Substructure of the outer dynein arm. *J. Cell Biol.* 95:798–815.
10. Goodenough, U. W., and J. E. Heuser. 1984. Structural comparison of purified dynein proteins with *in situ* dynein arms. *J. Mol. Biol.* 180:1083–1118.
11. Goodenough, U. W. 1983. Motile detergent-extracted cells of *Tetrahymena* and *Chlamydomonas*. *J. Cell Biol.* 96:1610–1621.
12. Bell, C. W., C. L. Fraser, W. S. Sale, W. Y. Tang, and I. R. Gibbons. 1982. Preparation and purification of dynein. *Methods Enzymol.* 85:450–474.
13. Heuser, J. E. 1983. Procedure for freeze-drying molecules adsorbed to mica flakes. *J. Mol. Biol.* 169:155–195.
14. Hopkins, J. M. 1970. Subsidiary components of the flagella of *Chlamydomonas reinhardii*. *J. Cell Sci.* 7:823–839.
15. Sale, W. S., and P. Satir. 1976. Splayed *Tetrahymena* cilia. A system for analyzing sliding and axonemal spoke arrangements. *J. Cell Biol.* 71:589–605.
16. Witman, G. B., J. Plummer, and G. Sander. 1978. *Chlamydomonas* flagellar mutants lacking radial spokes and central tubules. Structure, composition, and function of specific axonemal components. *J. Cell Biol.* 76:729–747.
17. Adams, G. M. W., B. Huang, G. Piperno, and D. J. L. Luck. 1981. Central-pair microtubular complex of *Chlamydomonas* flagella: polypeptide composition as revealed by analysis of mutants. *J. Cell Biol.* 91:69–76.
18. Gibbons, I. R., and A. V. Grimstone. 1960. On flagellar structure in certain flagellates. *J. Biophys. Biochem. Cytol.* 7:697–716.
19. Olson, G. E., and R. W. Linck. 1977. Observations of the structural components of flagellar axonemes and central pair microtubules from rat sperm. *J. Ultrastruct. Res.* 61:21–43.
20. Warner, F. D. 1981. Structure-function relationships in cilia and flagella. *In* Electron Microscopy of Proteins. J. R. Harris, editor. Academic Press, Ltd. London. 301–344.
21. Warner, F. D. 1970. New observations on flagellar fine structure. *J. Cell Biol.* 47:159–182.
22. Witman, G. B., R. Fay, and J. Plummer. 1976. *Chlamydomonas* mutants: evidence for the roles of specific axonemal components in flagellar movement. *In* Cell Motility. R. D. Goldman, T. O. Pollard, and J. L. Rosenbaum, editors. Cold Spring Harbor Laboratory, Cold Spring Harbor, N.Y. 969–986.
23. Warner, F. D. 1983. Organization of the interdoublet links in *Tetrahymena* cilia. *Cell Motility.* 3:321–332.
24. Tilney, L. G., J. Bryan, D. J. Bush, K. Fujiwara, M. S. Mooseker, D. B. Murphy, and D. H. Snyder. 1973. Microtubules: evidence for 13 protofilaments. *J. Cell Biol.* 59:267–275.
25. Haimo, L. T., B. R. Telzer, and J. L. Rosenbaum. 1979. Dynein binds to and crossbridges cytoplasmic microtubules. *Proc. Natl. Acad. Sci. USA.* 76:5759–5763.
26. Sale, W. S., U. W. Goodenough, and J. E. Heuser. 1984. The structure of dynein 1 of sea urchin sperm tail axonemes. *J. Cell Biol.* 99(4, Pt. 2):44a.
27. Johnson, K. A., and J. S. Wall. 1983. Structure and molecular weight of the dynein ATPase. *J. Cell Biol.* 96:669–678.
28. Goldstein, S. F. 1982. Motility of 9 + 0 mutants of *Chlamydomonas reinhardtii*. *Cell Motility.* 1 (Suppl.):165–168.
29. Baba, S. A. 1979. Regular steps in bending cilia during the effective stroke. *Nature (Lond.).* 282:717–720.
30. Gibbons, B. H., I. R. Gibbons, and B. Baccetti. 1983. Structure and motility of the 9 + 0 flagellum of eel spermatozoa. *J. Submicros. Cytol.* 15:15–20.